

Chaotic bubbling and nonstagnant foams

Alberto Tufaile*

*Escola de Artes, Ciências e Humanidades, Universidade de São Paulo, 03828-000, São Paulo, SP, Brazil
and Instituto de Física, Universidade de São Paulo, Caixa Postal 66318, 05315-970, São Paulo, SP, Brazil*

José Carlos Sartorelli

Instituto de Física, Universidade de São Paulo, Caixa Postal 66318, 05315-970, São Paulo, SP, Brazil

Philippe Jeandet and Gerard Liger-Belair

*Laboratoire d'Œnologie et Chimie Appliquée, UPRES EA 2069, URVVC, Faculté des Sciences de Reims,
Moulin de la Housse, B.P. 1039, 51687 Reims, Cedex 2, France*

(Received 18 January 2007; published 27 June 2007)

We present an experimental investigation of the agglomeration of bubbles obtained from a nozzle working in different bubbling regimes. This experiment consists of a continuous production of bubbles from a nozzle at the bottom of a liquid column, and these bubbles create a two-dimensional (2D) foam (or a bubble raft) at the top of this column. The bubbles can assemble in various dynamically stable arrangement, forming different kinds of foams in a liquid mixture of water and glycerol, with the effect that the bubble formation regimes influence the foam obtained from this agglomeration of bubbles. The average number of bubbles in the foam is related to the bubble formation frequency and the bubble mean lifetime. The periodic bubbling can generate regular or irregular foam, while a chaotic bubbling only generates irregular foam.

DOI: [10.1103/PhysRevE.75.066216](https://doi.org/10.1103/PhysRevE.75.066216)

PACS number(s): 05.45.Xt, 05.45.Gg, 05.45.Pq

I. INTRODUCTION

Bubble formation at a single orifice in a liquid column can be observed at a periodic, quasiperiodic, or chaotic behavior, following strict deterministic processes, and explained in the light of the dynamical systems. At the top of this column, these bubbles can last for a while, and form a foam. While many features such as drainage, film rupture, and liquid motion affect locally the bubble cluster evolution, the bubbling regime can dictate the foam geometry because the bubbles can assemble in various dynamically stable arrangements with different topologies, forming different kinds of foam structures. This is a typical phenomenon in which temporal processes at one place can generate structures in another place.

Foams represent examples of soft condensed matter in many physical-chemical processes, and understanding the motion of these gas bubbles and their respective clustering are problems of both scientific [1,2] and engineering importance [3,4]. However, the general knowledge of the dynamics of the bubble formation and its relationship with the nonstagnant foam is still limited because of the number of interacting phenomena that has to be taken into account, such as rapid bubble rupture, or its arrangement cannot always be reconciled with the usual two-dimensional models of foams, applicable mainly to stagnant foams, and consequently the dynamical process of bubbling connecting to the topological structure of foam is unclear.

In view of this, due to the fact that some archetypal pattern-forming scenarios can be produced naturally, such as hexagon packing in a glass of champagne [5], or by choosing

the experimental setup carefully, we have decided to focus on the foam obtained from a layer of ephemeral cohesive bubbles at the surface of a liquid column. The question here is “What are the main effects of different bubbling regimes in the foam shape?” We would like to determine how foam stability could be related by the different bubbling regimes.

In order to report our results, the next section presents the experimental apparatus, and in the other two sections we describe the different bubbling regimes and their influence in the foam structure, and the dynamical foam stability in the light of the bubble population balance, respectively.

II. EXPERIMENTAL APPARATUS

The diagram of Fig. 1(a) shows the bubbles rising in line and, at the surface of the column, the disengagement zone of the column, the bubbles leave the liquid bulk where they keep their integrity entrapped by thin liquid films creating the foam.

The bubble column consists of a cylindrical tube with an inner diameter of 11 cm and 70 cm in height. The bubbles are issued by injecting air through a metallic nozzle submerged in a viscous fluid (33% water and 67% glycerol), and the liquid is maintained at a level of 15 cm.

The nozzle is a hypodermic syringe needle (gauge 22) with an inner diameter of 0.4 mm, with a right angle tip cut with a length of 0.5 mm with a diamond saw, and it is placed with its tip 3.5 cm below the liquid surface. The nozzle is attached to a chamber with a capacity of 30 ml. Air from a compressor is injected to a capacitive reservoir, and a proportionating solenoid valve (Aalborg PSV-5) controlled by a proportional integral derivative (PID) controller sets the air flow to the chamber under the nozzle.

The flow rate is measured by a flowmeter Aalborg (GFM47). The pressure drop across the solenoid valve is

*Electronic address: tufaile@if.usp.br

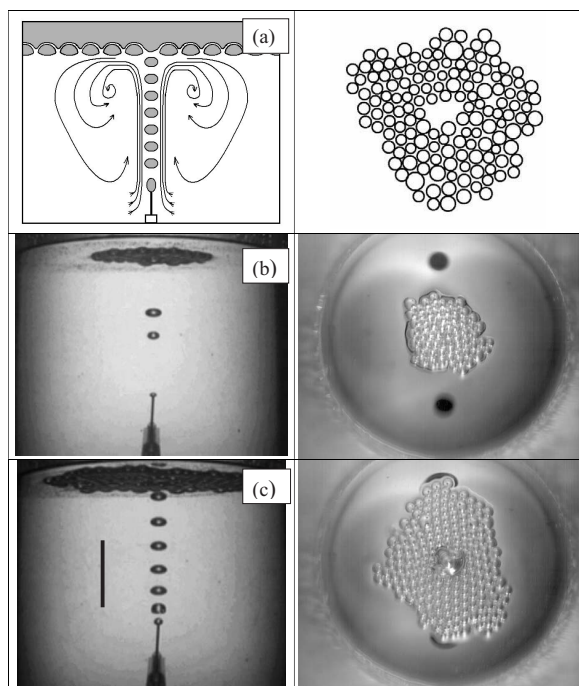


FIG. 1. (a) Experimental apparatus diagram with bubbles rising in line and the liquid motion, and the bubble cluster forming the foam from a top view of the interface of the liquid column. Experimental observation of some bubbling regimes and their respective foam: in (b) the bubbling in the period 3 with two bubbles rising in line, with the coalescence of the first two bubbles, and in (c) the bubbling in the period 1 in the regime of double coalescence close to the nozzle, and the respective foams. The length of each bar is 10 mm.

around 15 psi for the working range of air flow rate. In order to control the influence of the pneumatic system in the bubble formation dynamics, a tube is connected from the solenoid valve to the chamber under the nozzle, in which the tube inner diameter is 4.1 mm, and we used a length 50.0 cm long. Using a ramp function of the controller, the air flow rate ranged from 0 to 120 ml/min [6].

The detection system is based on a laser-photodiode system, with a horizontal diode laser beam focused in photodiode placed 2 mm above the nozzle. The time interval between successive bubbles is measured by a time circuitry inserted in a personal computer (PC) slot, with a time resolution equal to 1 μ s. The input signals are voltage pulses induced in a resistor, and defined by the beginning (ending) of scattering of a laser beam. The pulse width is the time interval t_n (n is the bubble number), and the time delay between two pulses defines the crossing time (dt_n) of a bubble through the laser beam, so that the total time interval is $T_n = t_n + dt_n$. Series of time intervals between bubbles $\{T_n\}$ were obtained, and then the bubble mean frequency was calculated as $f_b = 1/\langle T \rangle$. We estimated the total experimental noise around 100 μ s in the period 1 behavior. Using a camera with a high frame rate (500 per second), the FASTCAM-X1280PCI high-speed camera system connected to a PC, it is possible to observe the bubbling regimes and the foam shapes. Besides the images captured from the bubbles rising, we also obtained images of the foam from the upside, in

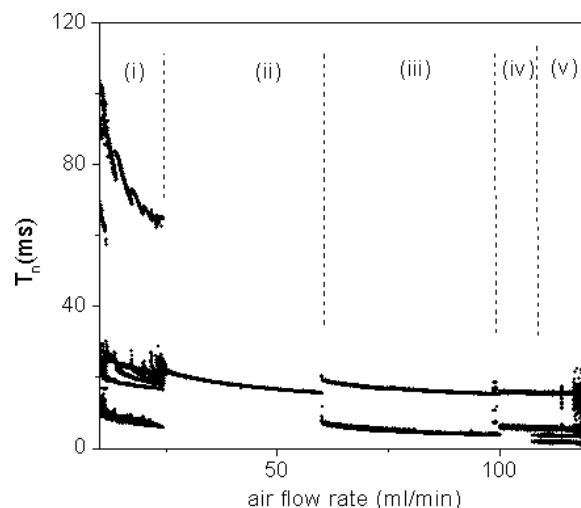


FIG. 2. Experimental bifurcation of the experiment showing the time interval T_n for 42 000 bubbles, while the increasing the flow rate from 0 to 120 ml/min, characterizing the bubbling regimes: (i) the period adding, (ii) the period 1, (iii) first coalescence in the period 2, (iv) second coalescence, and (v) the intermittent regime.

order to obtain their profiles in different bubbling regimes and foam shapes.

III. BUBBLING REGIMES AND FOAM STRUCTURE

To observe the influence of different types of bubbling regimes in the foam, we prepared the bubbling system working in a sequence of regimes and their respective foams viewing from the top, starting with the period-adding route to chaos [Fig. 1(b)], followed by the period 1 bubbling; after that there is a single coalescence regime, in which two consecutive bubbles coalesce close to the nozzle. The next case is the double coalescence regime shown in Fig. 1(c), forming a bigger bubble due to a cascade of the coalescence of four consecutive bubbles, and the intermittent regime involving periodic regimes and bursts. For each bubbling regime, we considered the regular foam for the case in which the bubbles have almost the same size, and the irregular foam containing bubbles with different sizes.

Using the air flow rate as the control parameter, the bubbling undergoes to the sequence of periodic bifurcations of k to $k+1$ periods, eventually separated with some chaotic regions, in a scenario known as period-adding route to chaos. This phenomenon was reported in previous papers, and compared to forced relaxation oscillators, in which an integrate-and-fire dynamics with a periodic threshold is related to a discontinuity or sharp derivative in the phase space obtained from a model [7–9]. The bifurcation diagram of the time interval T_n against the air flow rate of this bubbling regime is shown in Fig. 2(i). Furthermore, each periodic bubbling of this period-adding sequence generates bubble trains, with the coalescence of the two first bubbles of the train for periods higher than three, for air flow rates varying from 0 to 25 ml/min. This kind of dynamics generates bubbles with two sizes, the first one with twice the volume of the following bubbles. Generally an increasing in the air flow rate in

the period-adding regime causes an increasing in the number of the smaller bubbles in the foam. Occasionally some chaotic bubbling regimes can be found between two different periodic behaviors of this period-adding route. In the chaotic bubbling the bubble size distribution in the foam is very irregular. Therefore, the region represented in Fig. 2(i) just creates irregular foam, for any bubbling period higher than period 3, and the bubble formation is dependent on many parameters of the pneumatic system, such as the volume of the chamber under the nozzle, or the hose length connecting the air reservoir to the nozzle.

Increasing the air flow rate, the cascade of period adding ends abruptly through a tangential bifurcation to the period 1 stable regime in Fig. 2(ii) at the air flow rate of 25 ml/min. In this case, the bubbles are formed periodically, and after their detachment from the nozzle, they move upwards as single bubbles. Consequently, the bubble size in the foam obtained in this bubbling regime is roughly uniform, and consequently this single bubbling regime generates a mono-disperse foam, with a small number of defects compared to the previous cases. This regime indicates “constant pressure condition” in bubble formation, as it is called in the engineering jargon [10].

As the air flow rate is increased, the time between bubbles decreases, and for a critical value of the air flow rate of 60 ml/min, two consecutive bubbles coalesce near to the nozzle, forming a double bubble, with two time intervals represented by the sudden change of bubbling regime in Fig. 2(iii), creating a discontinuous bifurcation from period 1 to period 2 [6]. This bubbling regime also has the foam with a regular bubble size distribution, and the bubbles of this foam have twice the volume of the previous case.

Increasing the air flow rate more, the single coalescence occurs at smaller distances from the nozzle, decreasing the time between bubbles, for the next critical value of the air flow rate of 98 ml/min; the process of coalescence of two double bubbles occurs as regular as the single coalescence, and at this point a second discontinuous bifurcation of the bubble regime takes place [Fig. 2(iv)], affecting the foam the same way as the previous case. Figure 3 illustrates the details of some foams in order to compare the relative size of bubbles in each case. In Fig. 3(a) there is the image of the irregular foam from the chaotic bubbling, the regular foams in Fig. 3(b) from the period 1 bubbling, the single coalescence in Fig. 3(c), and in Fig. 3(d) we have the foam obtained from the double coalescence regime.

After the double coalescence there is a route to chaos via intermittency, when the air flow rate increases, in which the bubble train starts to pulsate intermittently around the air flow rate of 108 ml/min, and the sequence of bubbles launched periodically is interrupted by some irregular bursts. In Ref. [6] is obtained a transition to chaos via intermittency type III for this system. Increasing the air flow rate further, these irregular bursts become gradually more frequent. This bubbling regime also generates irregular foam.

In order to exemplify the nonlinearity involved in this system, the power spectra of the series of events of some bubbling regimes are shown in Fig. 4(a) for the air flow rate at 16.8 ml/min with a main peak at period 6, with subharmonics at period 2 and period 3. The chaotic bubbling near

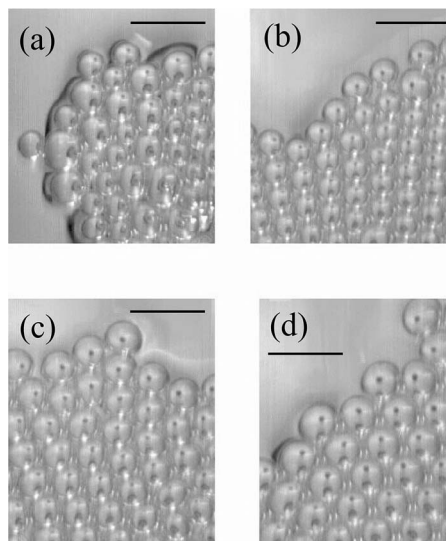


FIG. 3. Closeups of some foams obtained in (a) irregular foam from the chaotic bubbling with flow rate at 17 ml/min, (b) the regular foam obtained from a bubbling in the period 1 after the tangent bifurcation with air flow rate value of 27 ml/min, (c) the regular foam from the bubbling regime with the coalescence of two consecutive bubbles after the first discontinuous bifurcation at 73 ml/min, and (d) another regular foam obtained after the second coalescence regime at 103 ml/min. In these last three foams, the main feature is that above the coalescence point inside the liquid during the bubble formation, the coalesced bubbles again appear to have a period 1 pattern, and each bubble in the foam is two times larger than the previous case. The length of each bar is 10 mm.

the same period 6 bubbling at 17 ml/min is shown in Fig. 4(b) with several frequencies around the peaks of the previous case, and at 119 ml/min inside the intermittent regime is shown in Fig. 4(c) with broadband components.

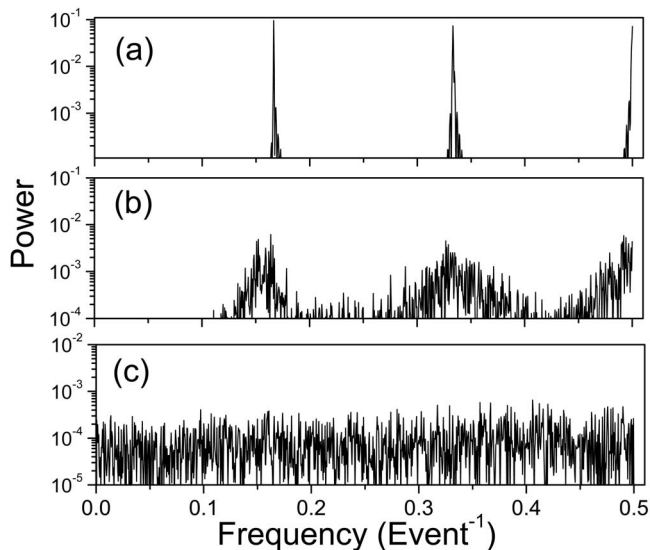


FIG. 4. The power spectra obtained from a period 6 bubbling is shown in (a) for the air flow rate at 16.8 ml/min, in (b) a chaotic bubbling near to this period 6 for the air flow rate at 17 ml/min, and in (c) a chaotic bubbling in the intermittent regime at 119 ml/min.

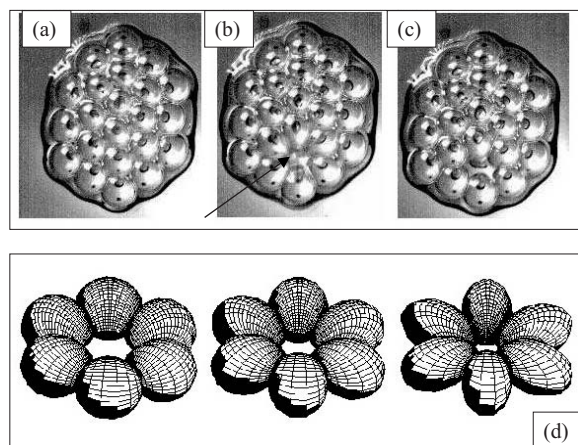


FIG. 5. The collapse of a bubble affecting its surrounding neighbors. These bubbles in touch with the collapsing ones experience shear stresses forming a “flower-shaped” structure, as is shown in time-sequence photographs of figures from (a) to (c), with the hole in the foam rapidly filled with neighboring bubbles, indicated by the arrow in (b). In (d) there is a schematic representation of the flower-shaped structure. The nozzle used to obtain only this foam was changed for a tube with 0.78 mm inner diameter to enhance the effect of bubble collapse.

IV. THE STABILITY OF THE FOAM

Now we turn to the stability of the foam. A regular bubble leaves the bulk of the liquid column at the center of the free surface, and moves toward the border of the foam pushed by the following bubbles, with the lifespan ranging from tenths of seconds to seconds, creating a bubble cluster with an irregular border around the center of the vessel. Generally speaking, the lifespan of a bubble emerging from a liquid depends on various factors, such as drainage of the liquid film in viscous fluids [11] and the lifetime of a bubble also depends on its length of travel through the liquid as it progressively collects tensioactive molecules along its way up, that in turn are able to increase the bubble’s lifetime by rigidifying the film of the emerged bubble cap [12].

In the present case there is a dynamic stability of the foam, consisting in a network of thin films involving interacting bubbles. The number of bubbles in the bubble raft is given by the balance between the generation and the destruction of the bubbles, creating a cohesive structure with a moving border. A direct observation of the foam reveals a relationship between the air flow rate and the size of this foam, besides the breaking events of bubbles occurring at random inside the foam. Even though the collapse of a bubble affects its surrounding neighbors, these bubbles adjacent to those which burst seldom collapse in turn, as already observed during the collapse of bubbles in a bubble monolayer at the surface of a liquid of low viscosity [13]. These bubbles in touch with the collapsing ones experience shear stresses forming a “flower-shaped” structure, as shown in time-sequence photographs of Figs. 5(a)–5(c), with a schematic representation of flower-shaped structures in Fig. 5(d). The bubble raft quickly rearranges itself to fill the hole left by the bursting bubble. This same general behavior is observed dur-

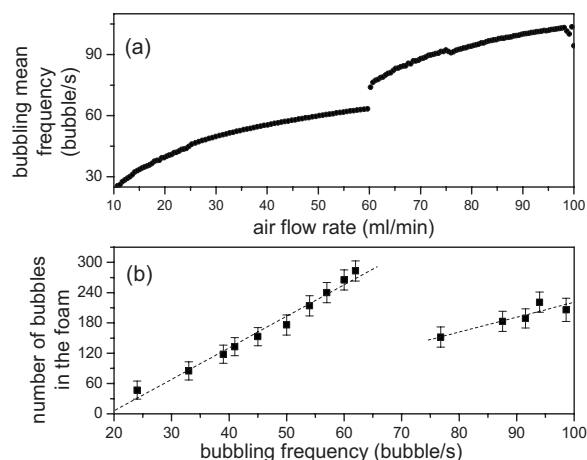


FIG. 6. The dependence between the bubbling frequency and the air flow rate is shown in (a), and in (b) is represented the plot of the number of bubbles and its relationship with the bubbling frequency. There is a linear dependence between these variables, interspersed by discontinuities due to coalescence during the bubble formation. The linear fit in each regime is represented by the dashed lines in each case is 6.23 s and 3.05 s.

ing the collapse of bubbles in a champagne bubble raft, as reported by Liger-Belair [5] (see, for example, from Fig. 28 to Fig. 36 in Ref. [5]). A different nozzle was used in order to enhance the observation of this effect.

If we consider the bubble population balance equation in a foam with N bubbles is given by

$$\frac{dN}{dt} = -DN + f_b, \quad (1)$$

in which D is the bubble-bursting rate coefficient and f_b is the bubbling frequency, the transient is

$$N(t) = N_0 e^{-Dt} + \frac{f_b}{D}. \quad (2)$$

For the case of a stable foam in which $dN/dt=0$ and $t \rightarrow \infty$ we obtain

$$N = \frac{1}{D} f_b. \quad (3)$$

In this way, the number of remaining bubbles in the foam also has a linear relation with the bubble frequency f_b , and is determined by the characteristic time scale $1/D$, which can be understood as the average value of the bubble lifespan in the foam.

The plot of Fig. 6(a) shows the data obtained from the experiment of the air flow rate against the mean bubble formation frequency. Initially the bubbling mean frequency increases up to 63 bubbles per second (16 ms), with the increase of the air flow rate until 60 ml/min. After that, there is a gap in the bubbling frequency at the flow rate of 61 ml/min showing a signature of the abrupt transition from the period 1 regime to single coalescence regime. There is no proportionality for all values between these two variables, so that the bubbling mean frequency is suddenly increased be-

cause the first bubble of the pair forming at the nozzle assumes an ellipsoidal shape, with a time of bubble formation around 18 ms, while the second bubble during its formation elongates in the vertical direction and coalesces in 7 ms, with a bubbling mean frequency around 80 bubbles/s, generating a larger coalesced bubble at each 25 ms (40 bubbles/s). The main consequence of this transition in the foam stability is an abrupt change of the bubble number N of the foam to drop to the half value of the bubble number in the previous period 1 bubbling. This argument highlights the advantage of understanding the mechanism using the bubbling frequency instead of the air flow rate, because the number of bubbles in the foam has a modular dependence with the bubbling mean frequency, and can be broken into pieces, and each piece can be analyzed separately by Eq. (3). The plot of Fig. 6(b) shows the data obtained from the experiment of the bubble formation frequency against the number of bubbles supporting this hypothesis, revealing that the relationship between these two variables is almost linear in the region corresponding to the period adding and the monotonous bubbling, corresponding to regions (i) and (ii) of Fig. 2. The value for the characteristic time scale obtained for the angular coefficient of the first dashed line in Fig. 6(b) is 6.23 s. The time scale changes to 3.05 s for the region of single coalescence in Fig. 6(b).

We also observed a second transition at the flow rate of 98 ml/min, from single to double coalescence, with the time scale value of 1.50 s for the foam obtained for the bubbling represented in regions (iv) and (v) of Fig. 2. Therefore, after each bubbling transition, as the air flow rate is increased, the bubble time scale is decreased almost by half.

V. CONCLUSIONS

We described the formation and bubble clustering at the top of a liquid column, obtained from a nozzle issuing bubbles at different bubbling regimes. Due to the fact that different bubble sizes generate irregular foam, bubbles obtained from period adding with multiple periods and chaotic bubbling are associated with irregular foam. Bubbling in period 1, or bubbling with multiple periods with the coalescence of the bubbles close to the nozzles creates monodisperse foam.

In this experiment, there is a limit to how many bubbles can occupy this two-dimensional foam simultaneously. Specifically, the number of bubbles in the foam is proportional to the bubbling frequency multiplied by the average value of bubble lifetime. Any discontinuity in this relationship is an effect of coalescing processes of bubbles close to the nozzle, which causes an abrupt change in the bubble size. We derived the stability of the foam from the equation that gives the balance between the generation and the destruction of bubbles, and obtained the average time that a bubble survives before it bursts in the foam, in which the number of remaining bubbles in the foam has a linear relationship with the bubble frequency.

ACKNOWLEDGMENTS

This work was supported by the Brazilian agency FAPESP and Instituto do Milênio de Fluidos Complexos (IMFCx-CNPq).

-
- [1] D. Weaire and S. Hutzler, *The Physics of Foams* (Clarendon Press, Oxford, 1999).
 - [2] N. Vandewalle, H. Caps, and S. Dorbolo, *Physica A* **314**, 320 (2002).
 - [3] A. A. Kulkarni and J. B. Joshi, *Ind. Eng. Chem. Res.* **44**, 5873 (2005).
 - [4] S. U. Sarnobat, S. Rajput, D. D. Bruns, D. W. DePaoli, C. S. Daw, and K. Nguyen, *Chem. Eng. Sci.* **59**, 247 (2004).
 - [5] G. Liger-Belair, *Uncorked: The Science of Champagne* (Princeton University Press, Princeton, 2004).
 - [6] A. Tufaile and J. C. Sartorelli, *Phys. Rev. E* **66**, 056204 (2002).
 - [7] V. S. M. Piassi, A. Tufaile, and J. C. Sartorelli, *Chaos* **14**, 477 (2004).
 - [8] E. Colli, V. S. M. Piassi, A. Tufaile, and J. C. Sartorelli, *Phys. Rev. E* **70**, 066215 (2004).
 - [9] G. Liger-Belair, A. Tufaile, B. Robillard, P. Jeandet, and J. C. Sartorelli, *Phys. Rev. E* **72**, 037204 (2005).
 - [10] R. Clift, J. Grace, and M. Weber, *Bubble, Drops and Particles* (Academic Press, New York, 1978).
 - [11] G. Debreges, P. G. De Gennes, and F. Brochart-Wyart, *Science* **279**, 1704 (1998).
 - [12] B. Jachimska, P. Warszynski, and K. Malysa, *Colloids Surf., A* **143**, 429 (1998).
 - [13] G. Liger-Belair and P. Jeandet, *Langmuir* **19**, 5771 (2003).